

Accounting for motion of supernova host galaxy in statistical inference from SNIa data

Ujjwal Upadhyay,^{a,b} Tarun Deep Saini,^a Shiv K. Sethi^b

^aDepartment of Physics, Indian Institute of Science, Bangalore, India

^bAstronomy and Astrophysics Group, Raman Research Institute, Bangalore, India

E-mail: ujjwalu@iisc.ac.in, tarun@iisc.ac.in, sethi@rri.res.in

Abstract. We investigate the impact of peculiar motion of Type Ia supernova host galaxies on cosmological parameter estimation. This motion causes their redshift to deviate from that of the comoving observer at their position and is a source of noise. To this end, we develop an estimator for parameter estimation in models with errors in independent variables. Using the Bayesian framework, errors in independent variables are treated as nuisance parameters by making the independent variables parameters of the model. Our method applied to the Pantheon sample of Type Ia supernova indicates a few percent shift in the central values of inferred cosmological parameters. For the w CDM model, we find that accounting for peculiar velocities makes the data marginally more consistent with the cosmological constant model. By using simulated data, we show that not accounting for peculiar velocities will significantly impact parameter estimation from higher precision future data sets.

Contents

1	Introduction	1
2	Methodology	3
2.1	Estimator for Errors-in-Variables	3
2.1.1	Estimator for nonlinear models	4
3	Magnitude–Redshift relation	6
4	Results	7
4.1	Application to Pantheon Data	8
4.2	Application to Synthetic Data	11
5	Conclusion and Discussion	12
A	Linear Approximation	13

1 Introduction

The spatially flat Λ CDM model, based on the cosmological principle of homogeneity and isotropy, constituting cold dark matter and the cosmological constant that dominates the universe at present, has become the standard description of our observed universe. It has been remarkably successful in describing the observed anisotropies in the Cosmic Microwave Background (CMB)[1], large-scale clustering of matter [2–4], and the background expansion history inferred from the redshift and brightness measurements of Type Ia supernovae (SNIa) [5–7]. In addition, a growing number of space and earth missions have ushered in the era of precision cosmology [8], which allows us to constrain cosmological parameters at a sub-percent level of precision. For example, the measurement of the CMB temperature and polarization anisotropies by the Planck mission has allowed us to constrain the Hubble constant within an uncertainty of 0.5 km/s/Mpc [1]. This increasing quality and quantity of data has enabled us to extract more detailed information about the present and past of the universe.

However, the onset of the era of greater precision has also revealed systematic discrepancies in the standard model of cosmology, such as the observed tensions in H_0 and S_8 [9–11]. Taking these discrepancies as a hint of new physics beyond the standard Λ CDM model, several modifications to the theory have been proposed in the literature, on the contrary, untreated or systematic errors in the analysis as a source of observed discrepancies remain a less explored but plausible alternative. For example, there are certain anomalies in the CMB observations, such as lensing anomalies, whose presence depends on the method used for statistical analysis. For example, the standard `Planck` and `Commander` likelihood of Planck 2018 data prefer a higher value of the lensing parameter A_L than the prediction of the Λ CDM model, $A_L = 1$. However, in the likelihood `NPIPE` based on the same Planck data but different modeling of systematics, there is no such anomaly [12]. It was shown in [13] that alleviating these tensions with extensions to the Λ CDM model is not sufficient to claim a hint for physics beyond the Λ CDM model. This also highlights the fact that increasing the precision in measurement

also requires more accurate statistical analysis techniques to obtain consistent results from different observational probes.

Although highly precise instrumentation equipped with artificial intelligence and machine learning is now widely used in astronomy, astronomical observations are never free from errors. These errors can originate from instrumental limitations, atmospheric interference (for ground-based telescopes), or cosmic background noise. Furthermore, systematic biases introduced during data processing and limitations of observational pipelines contribute to these inaccuracies. Despite this, while fitting a model to the data, it is very common to consider errors only on the main observable (dependent variable), treating subsidiary observables (independent variables) as perfectly measured. In part, this is due to the fact that the usual statistical techniques are based on the likelihood function that is derived from the errors in the main observable. This is usually justified if the errors in the subsidiary observables are small compared to the errors in the dependent variable.

In statistics literature, the study of model fitting when there are errors in both dependent and independent variables is called *errors-in-variables models* [14]. Many different methods have been proposed to deal with this issue if additional information can be obtained about the independent variable. The instrumental variable method [14] considers another variable that is related to the true regressor with some known relation. The method of repeated measurement [14] uses multiple observations of the same variable to minimize error. For the special case, when the model is a monotonic and differentiable function of the regressor variable, the likelihood can be written by inverting the model function [15]. However, there is no general method for fitting arbitrary errors-in-variable models.

In the context of cosmology, this issue could arise on various occasions. For example, it becomes relevant in estimating the cosmological parameters from the magnitude–redshift data of SNIa. Usually, the redshift determination of these supernovae is considered to be free of errors. There are at least two sources of errors in the determination of the redshift. Spectroscopic redshifts can be determined with a relative accuracy better than 10^{-4} . The second source of error arises from the line-of-sight peculiar velocities owing to gravitational interaction¹. The line-of-sight peculiar motion of host galaxies of supernovae contributes to the total observed redshift and cannot be disentangled from the contribution from cosmological expansion². From linear perturbation theory, the RMS of peculiar velocity varies from a few hundred km/sec to a few thousand km/sec for scales 1 Mpc to 100 Mpc. The modeling of the peculiar motion of individual objects requires taking into account nonlinear effects, which could further enhance this effect. The impact of peculiar velocities could be more than an order of magnitude larger than the instrumental uncertainty but still small compared to Hubble recessional velocities except in the nearby universe. The impact of peculiar motion on the cosmological parameters has been studied in the literature using N-Body simulations [19–22]. The peculiar velocity correction in the Pantheon+ SNIa sample was obtained in [23]. These studies focus mainly on the determination of the Hubble constant.

In this work, we analyze the impact of peculiar velocities on the determination of cosmological parameters using SNIa data by studying the problem of fitting models with errors in

¹Cosmological peculiar velocities are a key prediction of the gravitational collapse model of structure formation. Their impact can be detected in the redshift-space two-point correlation function of galaxies (e.g. [16] and the references therein for details). These velocities can also be detected statistically using the kSZ (Kinetic Sunyaev-Zeldovich) effect (e.g. [17, 18])

²The contribution of peculiar motion also arises from our motion with respect to the cosmic rest frame. The magnitude and direction of this component can be determined from the measurement of the CMB dipole. It is corrected for in the available SNIa data as in the Pantheon sample.

both dependent and independent variables. We analyze the Pantheon SNIa sample [24] using three estimators—one without peculiar motions, one based on a locally linear magnitude–redshift relationship, and finally, one that accounts for the theoretical model without any approximation. We then apply our estimators on simulated data with parameters (e.g. number of SNIa, errors on magnitude) typical of the current and future SNIa data sets. For our study, we consider two cosmological models: a spatially flat Λ CDM model and a w CDM model with constant w .

This paper is organized as follows. In Section 2, we discuss in general our method for dealing with the problem of fitting arbitrary models with errors in both variables. In Section 3, we present the magnitude–redshift relation as an errors-in-variables model. In Section 4, we apply this method to estimate cosmological parameters from supernova data for the Λ CDM and the w CDM model, and discuss the modification in the results as compared to the standard model fitting method that does not consider the contribution of peculiar motion. In Section 5, we conclude with a discussion of the results and potential future applications of our method. In Appendix A, we derive an expression for likelihood in the linear approximation of the magnitude–redshift relation.

2 Methodology

The problem of regression with an arbitrary errors-in-variables model is interesting and, to the best of our knowledge, not a commonly addressed problem in astronomy. Since astronomical data usually have errors in independent variables, this could have general applications in a variety of problems in astronomy. In this section, we describe a Bayesian approach to this problem. In Section 2.1, we describe our method in general while motivating our choice of the particular form of estimator that we propose. Then, in Section 3, we specialize it for the estimation of cosmological parameters from the magnitude–redshift data of the Pantheon sample of supernovae [24]. We consider the contribution of peculiar motion of supernova host galaxies to the redshift uncertainty, which leads to its formulation as an errors-in-variables problem. We also compare it to an approach that uses a local linear approximation of the magnitude–redshift relation and uses known methods of handling errors-in-variables for linear models.

2.1 Estimator for Errors-in-Variables

Quite often, the output of experiments is a pair (x_i, y_i) ³ of N data points with uncertainties, assuming the randomness to be Gaussian, σ_{x_i} and σ_{y_i} , associated with each observed value x_i and y_i respectively. The quantity y_i often depends on the independently measured quantity x_i through a model that could be given through a mathematical relation

$$y_i = f(\theta, x_i), \tag{2.1}$$

or, in general, could be given by an algorithm such as a numerical simulation or a complex mathematical operation. Here, $f(\theta, x_i)$ is a function of the m model parameters, $\theta \equiv (\theta_1, \theta_2, \dots, \theta_m)$ and the variable x_i . In our notation, if any expression depends explicitly on a single variable, then we notate it with a subscript; else, we use unscripted symbols to refer to them collectively. We shall soon focus on the case of apparent magnitude versus redshift

³It is worth noting that in general, the data could have several independent variables (x_i, y_i, z_i, \dots) . It is straightforward to generalize this analysis to such multivariate cases.

data that comprises the measured pair (z_i, m_i) , which might be helpful to the reader while reading the following discussion to make it less abstract.

If the function $f(\theta, x_j)$ is a linear function of x_j , then estimating the parameters θ from data that have errors on both axes is quite straightforward (see, for example, [25] and the derivation in Appendix A). This method is based on the conversion of the x error into the y error through the slope of the linear function and adding it in quadrature to the y error while constructing the likelihood function. However, when the model is nonlinear in x_j , this trick works only by approximating the fitting function as locally a linear function, as shown for the special case of the magnitude–redshift relation in the Appendix A. Although, in general, a nonlinear model could refer to nonlinear dependence on θ or x_i , in this paper, by nonlinear model, we always refer to the latter case.

2.1.1 Estimator for nonlinear models

To keep things general, let $P_Y(\epsilon_Y)$ be the probability distribution function for random statistical noise in the measurement of y , so that the observed values are offset from their true value by a random number, $y_i = f(\theta, x_i) + \epsilon_{Yi}$, where ϵ_{Yi} is the random error in the measurement y_i . Therefore, the likelihood function is given by

$$\mathcal{L}(\mathcal{D} | \theta) = \prod_i P_Y(y_i - f(\theta, x_i)), \quad (2.2)$$

where \mathcal{D} collectively refers to the pair (x, y) . In Bayesian statistics, using Bayes' theorem, this likelihood function can be used to write the posterior probability distribution for parameters θ as

$$P(\theta | \mathcal{D}; I) \propto \mathcal{L}(\mathcal{D} | \theta; I)P(\theta | I) \quad (2.3)$$

where $P(\theta | I)$ is the prior probability distribution function for θ , and the addition of I in various terms symbolizes all the prior information that we may have (for details, see, e.g., [26]). Until now, the variables x have been considered given and fixed. To incorporate error in variables x in the posterior distribution, we now turn them into undetermined parameters x^* , equivalent to parameters θ , in terms of which the likelihood function can be written as

$$\mathcal{L}(\mathcal{D} | \theta, x^*; I) = \prod_i P_Y(y_i - f(\theta, x_i^*)) \quad (2.4)$$

Note that conversion of x to parameter means that now the data \mathcal{D} refers only to y . The information about errors in x and their measured values can be brought into our analysis as a prior on x^* through⁴

$$P(x_i^* | I) = P_X(x_i^* - x_i),$$

where P_X is the probability distribution for errors in variable x (assumed for simplicity to be the same for all data points, but this can be easily generalized). The modified posterior distribution is given by

$$P(\theta, x^* | \mathcal{D}; I) \propto \prod_i P_Y(y_i - f(\theta, x_i^*))P(x_i^* | I)P(\theta | I) \quad (2.5)$$

If the random noise is Gaussian, then the log of the likelihood function is given by

⁴We can derive the same expressions by noting that the joint probability of errors ϵ_X and ϵ_Y is given by $P_X(\epsilon_X)P_Y(\epsilon_Y)$, thus the errors on x can be considered to be a part of likelihood of a data set comprising the pair (x, y)

$$\ln \mathcal{L}(\mathcal{D} | \theta, x^*) = -\frac{1}{2} \sum_{i=1}^N \left[\frac{y_i - f(\theta, x_i^*)}{\sigma_{y_i}} \right]^2 \equiv -\frac{\chi_Y^2(\theta, x^*)}{2}, \quad (2.6)$$

and the log of the prior probability distribution function for x is given by

$$\ln P(x_i^* | I) = -\frac{1}{2} \sum_{i=1}^N \left[\frac{x_i^* - x_i}{\sigma_{x_i}} \right]^2 \equiv -\frac{\chi_X^2(x^*)}{2} \quad (2.7)$$

In terms of these variables, the posterior distribution can be written as

$$P(\theta, x^* | \mathcal{D}) \propto \exp \left[-\frac{\chi_Y^2(\theta, x^*) + \chi_X^2(x^*)}{2} \right] P(\theta | I) \quad (2.8)$$

We can marginalize x^* to obtain the probability distribution for θ

$$P(\theta | \mathcal{D}) \propto \int d^N x^* \exp \left[-\frac{\chi_Y^2(\theta, x^*) + \chi_X^2(x^*)}{2} \right] P(\theta | I) \quad (2.9)$$

In practice, marginalization is more conveniently carried out through MCMC, as we discuss later.

Since the total number of parameters now exceeds the number of data points, there is, in principle, the possibility of overfitting the data. In order to obviate this possibility, we add a regularization term as a prior probability that our physical model should be such that the mean value of χ_Y^2 is close to degrees of freedom of the model⁵. For the case of Gaussian noise in the dependent variable, this is just the probability distribution function for χ_Y^2 given by

$$P_{\chi^2}(\chi_Y^2) = \frac{\chi_Y^{k-2} \exp(-\chi_Y^2/2)}{2^{k/2} \Gamma(k/2)}, \quad (2.10)$$

where $k = N - m$ is the desired degrees of freedom of the fit (not accounting for noise in the x values). For example, for the case of fitting luminosity distance to distant supernovae, this would be the total number of supernovae minus the number of cosmological parameters being fitted. Therefore, our final form for the posterior distribution function for θ can be obtained by multiplying it with the probability distribution function for χ_Y^2

$$P(\theta | \mathcal{D}) \propto \int d^N x^* \exp \left[-\frac{\chi_Y^2(\theta, x^*) + \chi_X^2(x^*)}{2} \right] P(\theta | I) P_{\chi^2}(\chi_Y^2). \quad (2.11)$$

Regularization is commonly used in fitting complex models with a large number of parameters as it acts as a constraint and facilitates stable maximization of the posterior distribution (e.g. [26]). However, as we note later, the addition or omission of this term may not always change the dimensionality of the fit, as explained further in the context of the specific cosmological application of this method presented in the paper.

⁵This expectation is technically true only for linear models, but holds quite well in general for small errors as models can then be roughly treated as locally linear.

3 Magnitude–Redshift relation

Although the measurement error in the observed redshift of a supernova host galaxy is negligibly small, due to the possible peculiar motion of the host galaxy with respect to an observer at rest with respect to the universe, their observed redshift is shifted with respect to the theoretical cosmological redshift that encodes the expansion history of the universe. To estimate this shift, we note that

$$\frac{\nu_0}{\nu_{\text{obs}}} = \frac{\nu_0}{\nu_{\text{com}}} \frac{\nu_{\text{com}}}{\nu_{\text{obs}}} \approx (1+z)(1+v_p/c) \approx 1+z+v_p/c \quad (3.1)$$

where ν_{obs} , ν_0 , and ν_{com} are the frequencies observed at earth, in the rest frame of the galaxy and a comoving observer at the position of the galaxy, and v_p is the component of velocity of a galaxy with respect to the comoving observer parallel to the line-of-sight from the observer to the supernova host galaxy. The approximation in the last equation assumes $v_p/c \ll 1$, so we can neglect the transverse Doppler effect. For small redshifts where this correction dominates, it suffices to ignore the zv_p/c term, leading to the final form.

Peculiar motions also cause beaming of light towards the observer, alter the observed flux, and cause additional k-correction (e.g. see [27] for the combined impact of all these effects on the number count). The first two effects act in concert, as an object moving towards an observer would appear closer and less redshifted. The standard analysis already takes into account measurement errors in the luminosity of an SNIa, and these errors are much larger than what we expect from the peculiar motion of host galaxies. However, this is not true for redshift measurement errors that, as already noted, are small compared to peculiar motions. At low redshifts, this effect is enhanced as peculiar redshift/blueshift can become comparable to the redshift of the host galaxy. As more and more supernovae are observed, the effective statistical error in luminosity distance reduces at any redshift due to statistical averaging. Thus, we need techniques that allow us to handle errors on redshift, even if they are small.

The luminosity distance versus redshift relation is usually expressed in terms of the apparent magnitude of distant supernovae. To apply the analysis given in the previous section, we set the redshift z_i equal to x_i and the apparent magnitude m_i to the function $f(\theta, x_i)$. The apparent magnitude m and the luminosity distance D_L of a supernova of known absolute magnitude M are related through

$$m = M + 5 \log \left(\frac{D_L}{\text{Mpc}} \right) + 25 . \quad (3.2)$$

For a flat Friedmann–Lemaître–Robertson–Walker universe, the luminosity distance of a source at redshift z can be expressed as

$$D_L = \frac{c(1+z)}{H_0} \int_0^z \frac{dz'}{h(z')}, \quad (3.3)$$

where the dimensionless Hubble parameter is given by

$$h(z) = \left[\Omega_M(1+z)^3 + \Omega_{\text{DE}}(1+z)^{3(1+w)} \right]^{1/2}, \quad (3.4)$$

where Ω_M and Ω_{DE} are the present-day matter and dark energy densities respectively. The dark energy and pressure are related through the parameter w through $p_{\text{DE}} = w\rho_{\text{DE}}$. If dark

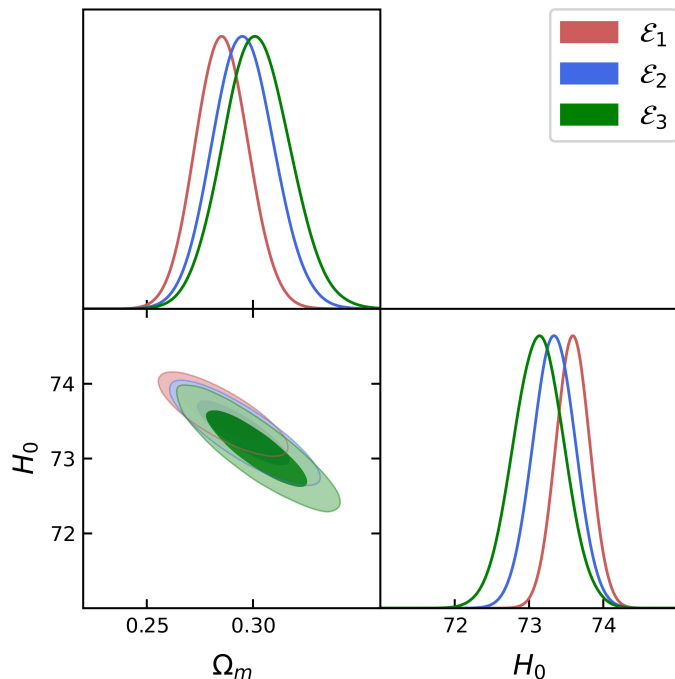


Figure 1. The figure displays one-dimensional posterior distributions and two-dimensional (1- and 2- σ) contours of Λ CDM parameters from Pantheon data using three different estimators. Estimator \mathcal{E}_1 (red) ignores any contribution to redshift from the peculiar motion of supernovae host galaxies, \mathcal{E}_2 considers it for the linearized model (see Appendix A for details), while \mathcal{E}_3 (green) represents our estimator, which incorporates the contribution from peculiar motion for the exact model.

energy is assumed to be the cosmological constant, then $w = -1$ in this parametrization. The apparent magnitude can be written as

$$m = M + 5 \log(cH_0^{-1}/\text{Mpc}) + 5 \log \left[(1+z) \int_0^z \frac{dz'}{h(z')} \right] + 25. \quad (3.5)$$

Here, w , Ω_M , and H_0 are free parameters of the model. However, note that H_0 is degenerate with M , which allows us to estimate only their combination.

4 Results

In cosmological studies, our primary concern is with the parameters w and Ω_M . For presenting our results, we need to marginalize various parameters, which means integrating them in the posterior distribution. Also note that in Eq. (2.11), we need to integrate over x^* , which corresponds to the redshift z in this case. Clearly, it is not feasible to integrate over so many variables. Therefore, to carry out marginalization, we employ the Markov Chain Monte Carlo (MCMC) sampling technique. Specifically, we develop and implement the Metropolis-Hastings algorithm within the MCMC framework to draw samples from the posterior distribution and use GetDist [28] python library for the analysis of MCMC samples.

Although distant SNIa are not ideal for determining H_0 due to degeneracy with M , in the following sections, we also present results for the Hubble parameter for the Λ CDM

Parameters	Priors	Best-fit values		
		\mathcal{E}_1	\mathcal{E}_2	\mathcal{E}_3
Ω_M	$\mathcal{U}(0.2, 0.4)$	0.286 ± 0.012	0.296 ± 0.014	0.302 ± 0.016
H_0	$\mathcal{U}(60, 80)$	73.59 ± 0.229	73.34 ± 0.287	73.13 ± 0.343

Table 1. The table presents results using Pantheon data for the spatially-flat Λ CDM model. It lists the priors, the best-fit values, and 1σ errors.

model. In order to break the aforementioned degeneracy, we use the absolute magnitude $M = -19.2478$ corresponding to the SHOES [29] value of $H_0 = 73.04$ km/s/Mpc for the Pantheon sample.

For the redshift error, we assume that each observed z_i in the data deviates from its true value z_i^* , which falls within a specified uncertainty range $z_i^* \in [z_i^{\min}, z_i^{\max}]$, where the min and max values are chosen to correspond to our assumptions about peculiar velocities. This is imposed even if we assume the distribution of redshift to be nonuniform. From analytical theory or numerical simulations, we can estimate the variance of galaxy peculiar velocities as a function of redshift. Also, note that only the line-of-sight component of the peculiar velocity contributes to the change in redshift. By the isotropy of the peculiar velocity dispersion, we have $\sigma_{v_{3D}} = \sqrt{3}\sigma_{v_p}$.

In our analysis below, we consider three distinct cases to present our results. The standard case is labeled as \mathcal{E}_1 , where we do not account for the redshift error. In Appendix A, we derive an estimator based on the linearized magnitude–redshift relation labeled \mathcal{E}_2 to include the redshift error using the likelihood function (Eq. (A.6)). This is of interest since the MCMC-based final estimator (\mathcal{E}_3) using the method described in Section 2.1.1 (Eqs. (2.2)–(2.11)), which includes the contribution of peculiar velocity to the observed redshift by treating each redshift as a parameter, can be computationally expensive for large data sets.

4.1 Application to Pantheon Data

We apply our method to fit the Λ CDM and the w CDM models to the magnitude–redshift data of Type Ia supernovae in the Pantheon sample [24]. This data set contains 1048 spectroscopically confirmed SNIa. For all cases, we run 12 independent MCMC chains for 10^6 steps. We use the Gelman-Rubin criterion of convergence. For the Λ CDM model, we achieve $R - 1 < 0.001$, while for the w CDM model it is $R - 1 < 0.005$. For z -errors, we use uniform priors for v_{pi} in the range: $-1000 \leq v_{pi} \leq 1000$ km s $^{-1}$ around the measured redshift. To verify convergence and test its rate, we increase the range of peculiar velocities to $-3000 \leq v_{pi} \leq 3000$ km s $^{-1}$. Increasing this interval reduces the acceptance rate and increases $R - 1$ for the fixed number of MCMC steps. However, $R - 1$ is always less than 0.01. Thus, it leads to slower convergence, but our results remain unchanged; we also obtain the same results by assuming a Gaussian distribution for peculiar velocities, imposing only the condition that $x^* > 0$.

It should be noted that our results are insensitive to regularization (Eq. (2.11)). The regularization term only changes the acceptance rate, indicating that the inclusion of redshift errors does not increase the dimensionality of our fitted physical model. This is not surprising if we note that overfitting requires the fitting function to be able to pass through most of the

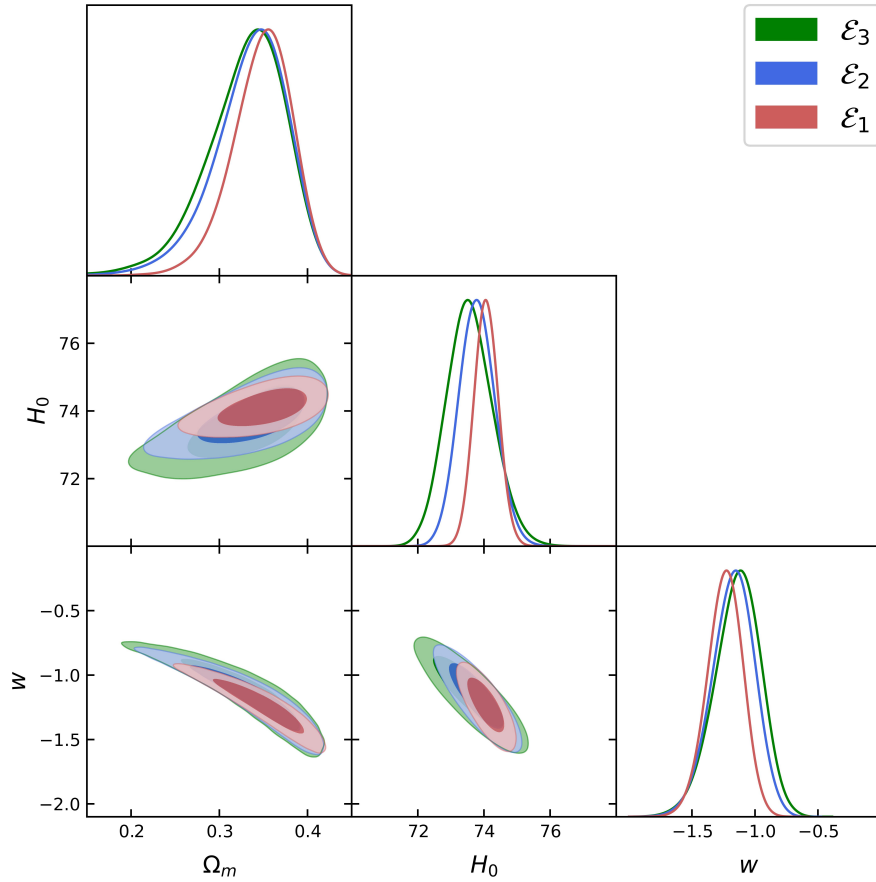


Figure 2. The figure shows posterior distributions and contours of w CDM parameters from Pantheon data using three different estimators. It follows the convention used in Figure 1.

Parameters	Priors	Best-fit values		
		\mathcal{E}_1	\mathcal{E}_2	\mathcal{E}_3
Ω_M	$\mathcal{U}(0.1, 0.6)$	0.348 ± 0.035	0.335 ± 0.043	0.330 ± 0.046
H_0	$\mathcal{U}(60, 80)$	74.07 ± 0.368	73.80 ± 0.546	73.58 ± 0.703
w	$\mathcal{U}(-2, 0)$	-1.24 ± 0.14	-1.17 ± 0.17	-1.14 ± 0.18

Table 2. The table presents results using Pantheon data for the spatially-flat w CDM model. It lists the priors, the best-fit values, and 1σ errors.

noisy data points. This would require the fitting function to have the flexibility that Eq. (3.2) does not have, even if we convert the redshift to a variable. The function remains a monotonic function of redshift and thus does not cause overfitting of the data.

Figures 1 and 2 display the posterior distribution and the confidence regions 1σ and 2σ

for the Λ CDM and w CDM models for the Pantheon data. Different colors represent the three different estimators used. The red color represents the standard case, \mathcal{E}_1 , blue represents the linearized estimator, \mathcal{E}_2 , and the green represents the MCMC estimator, \mathcal{E}_3 . In both cosmological models, we have assumed uniform priors for the cosmological parameters, which are listed in Tables 1 and 2. Perusal of Figures 1 & 2 indicates that accounting for peculiar velocities in the current data does not significantly change the estimated parameters. However, note that in Table 2 for the w CDM model, the marginalized estimate for the dark energy parameter w is found to be marginally more consistent with the Λ CDM model, indicating that even at the current level of precision, the data could indicate non-trivial dark energy if systematic errors in redshift are not corrected. As the number of supernovae increases, this correction is likely to become even more significant. Next, we consider simulated data to investigate this issue further.

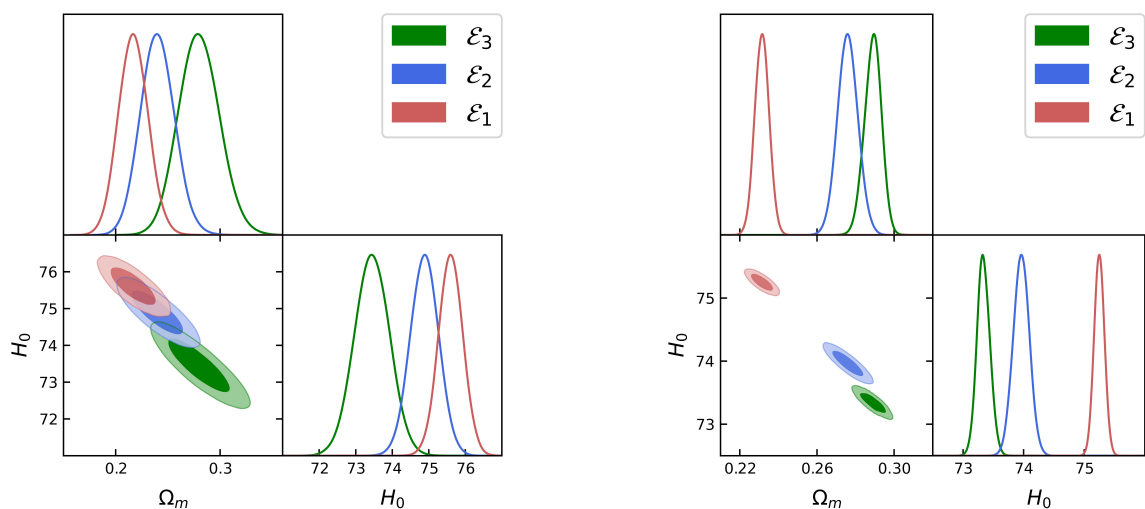


Figure 3. Constraints on the Λ CDM parameters from synthetic data with magnitude error $\Delta m = 0.2$ (left) and $\Delta m = 0.05$ (right) The colour scheme of Figure 1 is followed.

Models	Parameters	Priors	True values	Best-fit values		
				\mathcal{E}_1	\mathcal{E}_2	\mathcal{E}_3
Λ CDM	Ω_M	$\mathcal{U}(0.1, 0.5)$	0.30	0.217 ± 0.014	0.240 ± 0.016	0.280 ± 0.020
	H_0	$\mathcal{U}(60, 80)$	73.0	75.60 ± 0.338	74.88 ± 0.391	73.45 ± 0.482
w CDM	Ω_M	$\mathcal{U}(0.1, 0.5)$	0.30	0.368 ± 0.023	0.356 ± 0.028	0.320 ± 0.048
	H_0	$\mathcal{U}(60, 80)$	73.0	78.01 ± 0.642	77.09 ± 0.849	74.29 ± 1.024
	w	$\mathcal{U}(-3, 0)$	-1.0	-1.89 ± 0.213	-1.68 ± 0.236	-1.22 ± 0.228

Table 3. Priors and best-fit values for the Λ CDM and the w CDM parameters obtained from synthetic data with $\Delta m = 0.2$.

4.2 Application to Synthetic Data

For simulations, we first consider the parameters of the Pantheon sample: 1048 supernovae in the redshift range $z \in [0.01, 2.26]$ with magnitude errors, $\Delta m \simeq 0.2$ (for simulation, we assume Gaussian random errors, $\mathcal{N}(0, 0.20)$). We also consider a future SNIa project with errors four times smaller in magnitude, $\mathcal{N}(0, 0.05)$. This is possible with a sample 16 times larger than the Pantheon sample with the magnitude errors obtained from binning the data in redshift (this might be achieved with Zwicky Transient Facility (ZTF)[30] and the Large Synoptic Sky Survey Telescope (LSST) [31, 32], albeit with higher supernovae density at $z < 0.5$, see, e.g. [33] for details). The cosmological and other parameters are fixed to the following values: $\Omega_M = 0.30$, $H_0 = 73 \text{ km s}^{-1} \text{ Mpc}^{-1}$, $w = -1.0$, and the absolute magnitude of supernova, $M = -19.24$. To account for peculiar velocities, each supernova is assigned an error on its redshift, $\mathcal{U}(0, 0.003)$, drawn from a uniform distribution.

Our main results are shown in Figures 3 and 4 together with Tables 3 and 4. A comparison of the analysis of synthetic data with Figures 1 and 2 enables us to discern the following: (a) there is bias in the estimation of cosmological parameters using estimators \mathcal{E}_1 and \mathcal{E}_2 . The bias is larger if the peculiar velocity contribution is totally neglected (\mathcal{E}_1) and is partly alleviated if the linear approximation (Appendix A) is used and (b) while the overlapping confidence regions for $\Delta m = 0.2$ do not allow us to determine this bias unambiguously using the current data, the analysis of the future data without taking into account peculiar velocities of host galaxies will result in significant bias in the determination of cosmological parameters. In particular, the analysis of SNIa data without accounting for peculiar velocities could bias the nature of dark energy, an important issue from the point of view of both cosmology and theoretical physics, and much debated in recent times following DESI results (e.g. [4]).

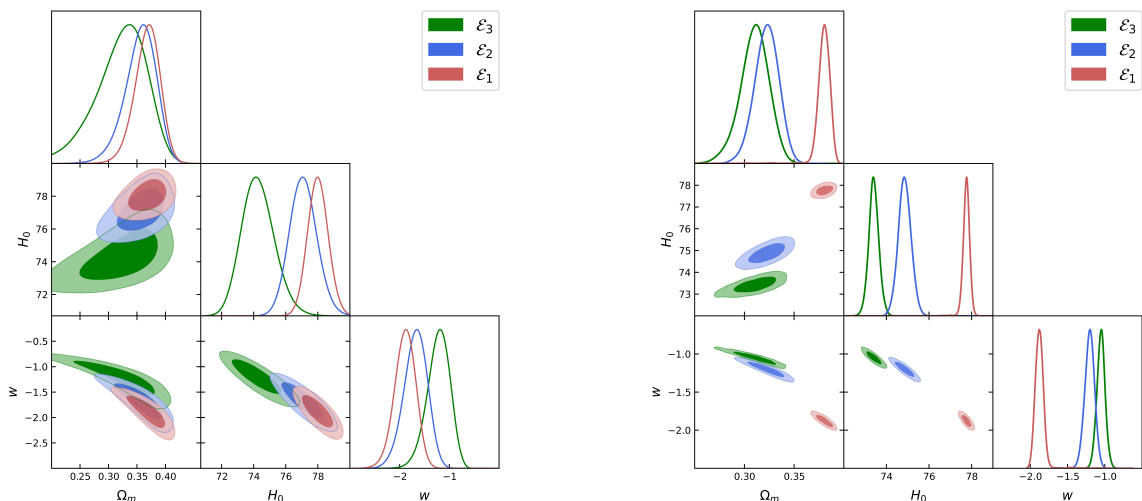


Figure 4. Constraints on the w CDM parameters from synthetic data with $\Delta m = 0.2$ (left) and $\Delta m = 0.05$ (right).

Models	Parameters	Priors	True values	Best-fit values		
				\mathcal{E}_1	\mathcal{E}_2	\mathcal{E}_3
Λ CDM	Ω_M	$\mathcal{U}(0.2, 0.4)$	0.30	0.233 ± 0.005	0.280 ± 0.005	0.298 ± 0.005
	H_0	$\mathcal{U}(60, 80)$	73.04	75.42 ± 0.19	74.03 ± 0.129	73.22 ± 0.118
w CDM	Ω_M	$\mathcal{U}(0.2, 0.4)$	0.30	0.38 ± 0.010	0.322 ± 0.012	0.310 ± 0.015
	H_0	$\mathcal{U}(60, 80)$	73.04	77.74 ± 0.252	74.86 ± 0.304	73.41 ± 0.243
	w	$\mathcal{U}(-3, 0)$	-1.0	-1.87 ± 0.08	-1.20 ± 0.07	-1.05 ± 0.06

Table 4. Priors and best-fit values for the Λ CDM and the w CDM parameters obtained from synthetic data with $\Delta m = 0.05$.

5 Conclusion and Discussion

Cosmology has become a precision science in the past few decades. This has been achieved by an unprecedented increase in both the quality and quantity of data—Planck CMB temperature and polarization maps, Large galaxy surveys such as SDSS, and the detection of thousands of SNIa, etc. This also means physical effects hitherto considered beyond the ability of astronomical instruments are well within reach. However, such rapid progress also requires one to constantly improve existing statistical techniques and develop new ones. This paper is an effort in that direction.

The aim of the paper is two-fold. First, we develop a general Bayesian method to analyse data with errors in both independent and dependent variables (discussed in detail in section 2.1.1). Second, we employ this statistical estimator to SNIa data to test its applicability, efficacy, and relevance to the current and future SNIa and other cosmological data sets. In particular, our aim is to discern the role of peculiar velocities of host galaxies of SNIa on the determination of cosmological parameters.

In Figures 1 and 2, we apply our proposed method on the Pantheon SNIa data for two cosmological models we employ for illustration. The figures show that the current data do not require us to account for the nonzero peculiar velocity of the SNIa host galaxies. We next apply our estimators on synthetic data, which partly confirms our results with Pantheon data, for parameters of the current data (Figures 3 and 4). However, we show that the future data (e.g. Zwicky Transient Facility (ZTF)[30] and the Large Synoptic Sky Survey Telescope (LSST) [31, 32]) will be very sensitive to peculiar velocities of SNIa host galaxies, and we would need appropriate statistical tools (section 2.1.1) to extract cosmological parameters from such a data set without bias (Figures 3 and 4).

One possible improvement of our work is more detailed modelling of peculiar velocities of host galaxies. It is difficult to predict the peculiar velocities of host galaxies without N-body simulations (e.g. [19] for a recent effort on the impact of peculiar velocities on Hubble’s constant measurement). This velocity would also depend on the location of host galaxies, e.g., a host galaxy in a rich cluster of galaxies as opposed to an isolated galaxy. In addition, and importantly, velocities are correlated across 100s of Mpc (e.g. [34] for details and further references), and this correlated component needs to be accounted for in a more detailed discussion (e.g. [33]). Also, the aim of our paper is to treat peculiar velocities as nuisance

parameters and to determine their impact on the interpretation of SNIa data. However, it is clear from the context that one might seek to infer cosmological peculiar velocities from the SNIa data. From cosmological data, peculiar flows are difficult to measure for individual objects and their presence is revealed through redshift-space distortion of galaxy correlation functions (e.g. [34] for details) and kSZ effect of clusters (e.g. [17, 18] for further details). Our proposed method might complement this ongoing effort to measure cosmological peculiar flows.

In future work, our aim is to extend our work with a better modeling of peculiar velocities along with studying the feasibility of their detection using the SNIa data. In addition, a combined analysis using SNIa data sets Pantheon+, DESY5, and Union3 might improve our results, which we hope to investigate in a later work. We also expect that our work will find general applicability in the analysis of other cosmological data sets, which we might study in upcoming works.

Acknowledgments

UU would like to acknowledge Yashi Tiwari for her valuable input throughout the project, particularly her insightful feedback on improving the efficiency of our Python code. UU also thanks Somnath Bharadwaj, Purba Mukherjee, and Avinash Paladi for their helpful comments.

A Linear Approximation

The problem of fitting errors-in-variable models is quite straightforward for linear models. This is because the linear model allows us to marginalize the likelihood over the true regressor analytically, resulting in a very simple likelihood that depends only on the observed values of the variables [25]. Since our model is not linear, we cannot apply it exactly. We compare our method with the standard method applied to the linear approximation of the model. Here, we derive an expression for the likelihood of the linear approximation of our model.

Apparent magnitude as a function of redshift, z , is given by

$$m(z) = M + 5 \log \left(\frac{D_L(z)}{\text{Mpc}} \right) + 25, \quad (\text{A.1})$$

where $D_L(z)$ is the luminosity distance given by,

$$D_L(z) = (1+z) \int_0^z \frac{c \, dz}{H(z)}. \quad (\text{A.2})$$

Considering errors in the measurement of both the apparent magnitude, m , and redshift, z , the likelihood can be expressed as

$$\ln \mathcal{L} = -\frac{1}{2} \sum_{i=1}^N \left(\frac{m_i - m(z_i^*)}{\sigma_{m_i}} \right)^2 - \frac{1}{2} \sum_{i=1}^N \left(\frac{z_i - z_i^*}{\sigma_{z_i}} \right)^2 \quad (\text{A.3})$$

This likelihood cannot be used to constrain the parameters of the model from the data since we do not have the true redshift values z_* , only the observed values z . Taylor expanding

the apparent magnitude about the observed redshift and keeping terms up to linear order in redshift, we can write

$$m(z^*) = m(z) + m'(z)(z^* - z) \quad (\text{A.4})$$

where $m'(z)$ is the derivative of $m(z^*)$ w.r.t. z^* evaluated at $z^* = z$, and is given by

$$m'(z) = \frac{5}{\ln 10} \left[\frac{1}{1+z} + \frac{1}{H(z) \int_0^z \frac{dz^*}{H(z^*)}} \right] \quad (\text{A.5})$$

With the above approximation, eq. (A.4), the likelihood takes the form,

$$\ln \mathcal{L} = -\frac{1}{2} \sum_{i=1}^N \left(\frac{m_i - m(z_i)}{\sigma_{m_i}} \right)^2 - \frac{1}{2} \sum_{i=1}^N \left[\left(\frac{m'^2(z_i)}{\sigma_{m_i}^2} + \frac{1}{\sigma_{z_i}^2} \right) (z_i^* - z_i)^2 - \frac{m'(m_i - m(z_i))}{\sigma_{m_i}^2} (z_i^* - z_i) \right]$$

Integrating over the true but unknown redshift z^* using the standard Gaussian integral, we obtain the marginalized likelihood,

$$\ln \mathcal{L} = -\frac{1}{2} \sum_{i=1}^N \frac{(m_i - m(z_i))^2}{\sigma_{m_i}^2 + m'^2(z_i) \sigma_{z_i}^2} \quad (\text{A.6})$$

Now, the likelihood depends only on the observed data. If we do not know the values of σ_{z_i} , as in our case, we can fix it at some value or make it a parameter. In this work, we chose to fix it at $\sigma_z = 0.003$, which corresponds to the peculiar velocity of 1000 km/s.

References

- [1] **Planck** Collaboration, N. Aghanim et al., *Planck 2018 results. VI. Cosmological parameters*, *Astron. Astrophys.* **641** (2020) A6, [[arXiv:1807.06209](#)]. [Erratum: *Astron. Astrophys.* 652, C4 (2021)].
- [2] **DES** Collaboration, J. Kwan et al., *Cosmology from large-scale galaxy clustering and galaxy-galaxy lensing with Dark Energy Survey Science Verification data*, *Mon. Not. Roy. Astron. Soc.* **464** (2017), no. 4 4045–4062, [[arXiv:1604.07871](#)].
- [3] **2dFGRS** Collaboration, S. Cole et al., *The 2dF Galaxy Redshift Survey: Power-spectrum analysis of the final dataset and cosmological implications*, *Mon. Not. Roy. Astron. Soc.* **362** (2005) 505–534, [[astro-ph/0501174](#)].
- [4] **DESI** Collaboration, A. G. Adame, J. Aguilar, S. Ahlen, S. Alam, D. M. Alexander, C. Allende Prieto, M. Alvarez, O. Alves, A. Anand, U. Andrade, E. Armengaud, S. Avila, A. Aviles, H. Awan, B. Bahr-Kalus, S. Bailey, C. Baltay, A. Bault, J. Behera, S. BenZvi, F. Beutler, D. Bianchi, C. Blake, R. Blum, M. Bonici, S. Brieden, A. Brodzeller, D. Brooks, E. Buckley-Geer, E. Burtin, R. Calderon, R. Canning, A. Carnero Rosell, R. Cereskaite, J. L. Cervantes-Cota, S. Chabanier, E. Chaussidon, J. Chaves-Montero, D. Chebat, S. Chen, X. Chen, T. Claybaugh, S. Cole, A. Cuceu, T. M. Davis, K. Dawson, A. de la Macorra, A. de Mattia, N. Deiosso, A. Dey, B. Dey, Z. Ding, P. Doel, J. Edelman, S. Eftekhari, D. J. Eisenstein, W. Elbers, A. Elliott, P. Fagrellius, K. Fanning, S. Ferraro, J. Ereza, N. Findlay, B. Flaugher, A. Font-Ribera, D. Forero-Sánchez, J. E. Forero-Romero, C. S. Frenk, C. Garcia-Quintero, L. H. Garrison, E. Gaztañaga, H. Gil-Marín, S. G. A. Gontcho, A. X. Gonzalez-Morales, V. Gonzalez-Perez, C. Gordon, D. Green, D. Gruen, R. Gspaner, G. Gutierrez, J. Guy, B. Hadzhiyska, C. Hahn, M. M. S. Hanif, H. K. Herrera-Alcantar, K. Honscheid, C. Howlett, D. Huterer, V. Iršič, M. Ishak, R. Joyce, S. Juneau, N. G. Karaçaylı,

- R. Kehoe, S. Kent, D. Kirkby, H. Kong, S. E. Kuposov, A. Kremin, A. Krolewski, O. Lahav, Y. Lai, T. W. Lan, M. Landriau, D. Lang, J. Lasker, J. M. Le Goff, L. Le Guillou, A. Leauthaud, M. E. Levi, T. S. Li, K. Lodha, C. Magneville, M. Manera, D. Margala, P. Martini, W. Matthewson, M. Maus, P. McDonald, L. Medina-Varela, A. Meisner, J. Mena-Fernández, R. Miquel, J. Moon, S. Moore, J. Moustakas, N. Mudur, E. Mueller, A. Muñoz-Gutiérrez, A. D. Myers, S. Nadathur, L. Napolitano, R. Neveux, J. A. Newman, N. M. Nguyen, J. Nie, G. Niz, H. E. Noriega, N. Padmanabhan, E. Paillas, N. Palanque-Delabrouille, J. Pan, S. Penmetsa, W. J. Percival, M. M. Pieri, M. Pinon, C. Poppett, A. Porredon, F. Prada, A. Pérez-Fernández, I. Pérez-Ràfols, D. Rabinowitz, A. Raichoor, C. Ramírez-Pérez, S. Ramirez-Solano, M. Rashkovetskyi, C. Ravoux, M. Rezaie, J. Rich, A. Rocher, C. Rockosi, N. A. Roe, A. Rosado-Marin, A. J. Ross, G. Rossi, R. Ruggeri, V. Ruhlmann-Kleider, L. Samushia, E. Sanchez, C. Saulder, E. F. Schlafly, D. Schlegel, M. Schubnell, H. Seo, A. Shafieloo, R. Sharples, J. Silber, A. Slosar, A. Smith, D. Sprayberry, T. Tan, G. Tarlé, P. Taylor, S. Trusov, R. Vaisakh, D. Valcin, F. Valdes, G. Valogiannis, M. Vargas-Magaña, L. Verde, M. Walther, B. Wang, M. S. Wang, B. A. Weaver, N. Weaverdyck, R. H. Wechsler, D. H. Weinberg, M. White, and M. J. Wilson, *DESI 2024 VII: Cosmological Constraints from the Full-Shape Modeling of Clustering Measurements*, *arXiv e-prints* (Nov., 2024) arXiv:2411.12022, [[arXiv:2411.12022](#)].
- [5] A. Conley, J. Guy, M. Sullivan, N. Regnault, P. Astier, C. Bolland, S. Basa, R. Carlberg, D. Fouchez, D. Hardin, et al., *Supernova constraints and systematic uncertainties from the first three years of the supernova legacy survey*, *The Astrophysical Journal Supplement Series* **192** (2010), no. 1 1.
- [6] D. Brout, D. Scolnic, B. Popovic, A. G. Riess, A. Carr, J. Zuntz, R. Kessler, T. M. Davis, S. Hinton, D. Jones, W. D. Kenworthy, E. R. Peterson, K. Said, G. Taylor, N. Ali, P. Armstrong, P. Charvu, A. Dwomoh, C. Meldorf, A. Palmese, H. Qu, B. M. Rose, B. Sanchez, C. W. Stubbs, M. Vincenzi, C. M. Wood, P. J. Brown, R. Chen, K. Chambers, D. A. Coulter, M. Dai, G. Dimitriadis, A. V. Filippenko, R. J. Foley, S. W. Jha, L. Kelsey, R. P. Kirshner, A. Möller, J. Muir, S. Nadathur, Y.-C. Pan, A. Rest, C. Rojas-Bravo, M. Sako, M. R. Siebert, M. Smith, B. E. Stahl, and P. Wiseman, *The Pantheon+ Analysis: Cosmological Constraints*, *ApJ* **938** (Oct., 2022) 110, [[arXiv:2202.04077](#)].
- [7] D. Scolnic, D. Brout, A. Carr, A. G. Riess, T. M. Davis, A. Dwomoh, D. O. Jones, N. Ali, P. Charvu, R. Chen, E. R. Peterson, B. Popovic, B. M. Rose, C. M. Wood, P. J. Brown, K. Chambers, D. A. Coulter, K. G. Dettman, G. Dimitriadis, A. V. Filippenko, R. J. Foley, S. W. Jha, C. D. Kilpatrick, R. P. Kirshner, Y.-C. Pan, A. Rest, C. Rojas-Bravo, M. R. Siebert, B. E. Stahl, and W. Zheng, *The Pantheon+ Analysis: The Full Data Set and Light-curve Release*, *ApJ* **938** (Oct., 2022) 113, [[arXiv:2112.03863](#)].
- [8] M. S. Turner, *The Road to Precision Cosmology*, [arXiv:2201.04741](#).
- [9] E. Di Valentino et al., *Snowmass2021 - Letter of interest cosmology intertwined II: The hubble constant tension*, *Astropart. Phys.* **131** (2021) 102605, [[arXiv:2008.11284](#)].
- [10] E. Di Valentino et al., *Cosmology Intertwined III: $f\sigma_8$ and S_8* , *Astropart. Phys.* **131** (2021) 102604, [[arXiv:2008.11285](#)].
- [11] E. Abdalla et al., *Cosmology intertwined: A review of the particle physics, astrophysics, and cosmology associated with the cosmological tensions and anomalies*, *JHEAp* **34** (2022) 49–211, [[arXiv:2203.06142](#)].
- [12] E. Rosenberg, S. Gratton, and G. Efstathiou, *CMB power spectra and cosmological parameters from Planck PR4 with CamSpec*, *Mon. Not. Roy. Astron. Soc.* **517** (2022), no. 3 4620–4636, [[arXiv:2205.10869](#)].
- [13] M. Cortès and A. R. Liddle, *On data set tensions and signatures of new cosmological physics*, *Mon. Not. Roy. Astron. Soc.* **531** (2024), no. 1 L52–L56, [[arXiv:2309.03286](#)].

- [14] C. Dougherty, *Introduction to Econometrics*. Oxford University Press, 2007.
- [15] P. Gregory, *Bayesian Logical Data Analysis for the Physical Sciences: A Comparative Approach with Mathematica® Support*. Cambridge University Press, 2005.
- [16] S. Dodelson and F. Schmidt, *The concordance model of cosmology*, in *Modern Cosmology*, pp. 1–19. Elsevier, 2021.
- [17] Planck Collaboration, N. Aghanim, Y. Akrami, M. Ashdown, J. Aumont, C. Baccigalupi, M. Ballardini, A. J. Banday, R. B. Barreiro, N. Bartolo, S. Basak, R. Battye, K. Benabed, J. P. Bernard, M. Bersanelli, P. Bielewicz, J. R. Bond, J. Borrill, F. R. Bouchet, C. Burigana, E. Calabrese, J. Carron, H. C. Chiang, B. Comis, D. Contreras, B. P. Crill, A. Curto, F. Cuttaia, P. de Bernardis, A. de Rosa, G. de Zotti, J. Delabrouille, E. Di Valentino, C. Dickinson, J. M. Diego, O. Doré, A. Ducout, X. Dupac, F. Elsner, T. A. Enßlin, H. K. Eriksen, E. Falgarone, Y. Fantaye, F. Finelli, F. Forastieri, M. Frailis, A. A. Fraisse, E. Franceschi, A. Frolov, S. Galeotta, S. Galli, K. Ganga, M. Gerbino, K. M. Górski, A. Gruppuso, J. E. Gudmundsson, W. Handley, F. K. Hansen, D. Herranz, E. Hivon, Z. Huang, A. H. Jaffe, E. Keihänen, R. Keskitalo, K. Kiiveri, J. Kim, T. S. Kisner, N. Krachmalnicoff, M. Kunz, H. Kurki-Suonio, J. M. Lamarre, A. Lasenby, M. Lattanzi, C. R. Lawrence, M. Le Jeune, F. Levrier, M. Liguori, P. B. Lilje, V. Lindholm, M. López-Cañiego, P. M. Lubin, Y. Z. Ma, J. F. Macías-Pérez, G. Maggio, D. Maino, N. Mandolesi, A. Mangilli, P. G. Martin, E. Martínez-González, S. Matarrese, N. Mauri, J. D. McEwen, A. Melchiorri, A. Mennella, M. Migliaccio, M. A. Miville-Deschênes, D. Molinari, A. Moneti, L. Montier, G. Morgante, P. Natoli, C. A. Oxborrow, L. Pagano, D. Paoletti, B. Partridge, O. Perdereau, L. Perotto, V. Pettorino, F. Piacentini, S. Plaszczynski, L. Polastri, G. Polenta, J. P. Rachen, B. Racine, M. Reinecke, M. Remazeilles, A. Renzi, G. Rocha, G. Roudier, B. Ruiz-Granados, M. Sandri, M. Savelainen, D. Scott, C. Sirignano, G. Sirri, L. D. Spencer, L. Stanco, R. Sunyaev, J. A. Tauber, D. Tavagnacco, M. Tenti, L. Toffolatti, M. Tomasi, M. Tristram, T. Trombetti, J. Valiviita, F. Van Tent, P. Vielva, F. Villa, N. Vittorio, B. D. Wandelt, I. K. Wehus, A. Zacchei, and A. Zonca, *Planck intermediate results. LIII. Detection of velocity dispersion from the kinetic Sunyaev-Zeldovich effect*, *A&A* **617** (Sept., 2018) A48, [[arXiv:1707.00132](#)].
- [18] H. Tanimura, S. Zaroubi, and N. Aghanim, *Direct detection of the kinetic Sunyaev-Zel’dovich effect in galaxy clusters*, *A&A* **645** (Jan., 2021) A112, [[arXiv:2007.02952](#)].
- [19] S. Gavas, J. S. Bagla, and N. Khandai, *Dispersion in the Hubble-Lemaître constant measurements from gravitational clustering*, [arXiv:2407.10139](#).
- [20] H.-Y. Wu and D. Huterer, *Sample variance in the local measurements of the Hubble constant*, *Mon. Not. Roy. Astron. Soc.* **471** (2017), no. 4 4946–4955, [[arXiv:1706.09723](#)].
- [21] R. Wojtak, A. Knebe, W. A. Watson, I. T. Iliev, S. Heß, D. Rapetti, G. Yepes, and S. Gottlöber, *Cosmic variance of the local Hubble flow in large-scale cosmological simulations*, *Mon. Not. Roy. Astron. Soc.* **438** (2014), no. 2 1805–1812, [[arXiv:1312.0276](#)].
- [22] E. R. Peterson et al., *The Impact from Galaxy Groups on Cosmological Measurements with Type Ia Supernovae*, [arXiv:2408.14560](#).
- [23] L. Giani, C. Howlett, K. Said, T. Davis, and S. Vagnozzi, *An effective description of Laniakea: impact on cosmology and the local determination of the Hubble constant*, *JCAP* **01** (2024) 071, [[arXiv:2311.00215](#)].
- [24] **Pan-STARRS1** Collaboration, D. M. Scolnic et al., *The Complete Light-curve Sample of Spectroscopically Confirmed SNe Ia from Pan-STARRS1 and Cosmological Constraints from the Combined Pantheon Sample*, *Astrophys. J.* **859** (2018), no. 2 101, [[arXiv:1710.00845](#)].
- [25] W. H. Press, B. P. Flannery, S. A. Teukolsky, and W. T. Vetterling, *Numerical Recipes in C: The Art of Scientific Computing*. second ed., 1992.

- [26] D. S. Sivia, *Data Analysis: A Bayesian Tutorial*. Oxford Science Publications. Oxford University Press, New York, 1996.
- [27] G. F. R. Ellis and J. E. Baldwin, *On the expected anisotropy of radio source counts*, *MNRAS* **206** (Jan., 1984) 377–381.
- [28] A. Lewis, *GetDist: a Python package for analysing Monte Carlo samples*, [arXiv:1910.13970](https://arxiv.org/abs/1910.13970).
- [29] A. G. Riess et al., *A Comprehensive Measurement of the Local Value of the Hubble Constant with 1 km s⁻¹ Mpc⁻¹ Uncertainty from the Hubble Space Telescope and the SH0ES Team*, *Astrophys. J. Lett.* **934** (2022), no. 1 L7, [[arXiv:2112.04510](https://arxiv.org/abs/2112.04510)].
- [30] M. J. Graham et al., *The Zwicky Transient Facility: Science Objectives*, *Publ. Astron. Soc. Pac.* **131** (2019), no. 1001 078001, [[arXiv:1902.01945](https://arxiv.org/abs/1902.01945)].
- [31] **LSST Science, LSST Project** Collaboration, P. A. Abell et al., *LSST Science Book, Version 2.0*, [arXiv:0912.0201](https://arxiv.org/abs/0912.0201).
- [32] **LSST** Collaboration, v. Ivezić et al., *LSST: from Science Drivers to Reference Design and Anticipated Data Products*, *Astrophys. J.* **873** (2019), no. 2 111, [[arXiv:0805.2366](https://arxiv.org/abs/0805.2366)].
- [33] K. Garcia, M. Quartin, and B. B. Sifert, *On the amount of peculiar velocity field information in supernovae from LSST and beyond*, *Physics of the Dark Universe* **29** (Sept., 2020) 100519, [[arXiv:1905.00746](https://arxiv.org/abs/1905.00746)].
- [34] S. Dodelson and F. Schmidt, *Modern Cosmology*. 2020.